OPERATION OF THE KEK 20 MEV INJECTOR LINAC

J. Tanaka, H. Baba, I. Sato, S. Inagaki, S.Anami, T. Kakuyama, T. Takenaka, Y. Terayama, H. Matsumoto
National Laboratory for High Energy Physics
Oho-Machi, Tsukuba-Gun, Ibaraki, Japan

Summary

A general description of the operational behavior of the KEK 20 MeV Injector linac will be given. Copper platings on the drift tubes and the inner surface of the tank have been great advantage to the high power rf excitation. The buncher debuncher and beam loading compensation system have been operated successfully. The maximum beam current of 150 mA was accelerated so far. The energy spread was less than ±1 % without debuncher and ±0.3 % with debuncher at the emittance of 0.6 πcm mrad and beam current of 120 mA. This paper also includes the experimental and calculated results of tilting of the tank field distribution.

Introduction

The KEK proton linac accelerated the first beam to 20 MeV on Aug.1, 1974. During the first 6 months the current level of the linac increased from several mA to several tens mA, and reached to maximum current of 94 mA in Jul. 1975. Since Nov.1974 the linac has served as the injector for the 500 MeV booster and 12 GeV main ring synchrotron. In Jan. 1976, the insulator of No.64 drift tube quadrupole magnet was broken due to accidental increasing of the trigger pulses more than two times which are generated from the booster. At the same time, the other several drift tube quadrupole magnets were also degraded their insulations. Owing to the accident the output current level decreased by 20 percent. However, the linac has continued the operation to the end of Mar. 1976, and eventually the main ring succeeded the acceleration of 10.4 GeV beam on Mar.19.

During the shut-down period from Apr. to May of this year the degraded drift tubes were replaced by new drift tubes.

In the end of May 1976, the linac started again the operation. The output current level increased up to 150 mA due to the improvement of the extractor of the ion source. Since that time the linac has been routinely operated at the current level of more than 100 mA. The design parameters and operational performances up to date are listed in Table I.

Table I

	Design	Operation	Best
Injection energy (MeV)	0.75	0.75	
Output energy (MeV)	20.5	20.3	
Peak current (mA)	100	100 ~ 120	150
Beam pulse length (μs)	0.6 ~ 30	15	
Energy spread (%)			
without Debuncher	<1.0	±1.2 at 120 mA	
with Debuncher	<0.5	±0.4	±0.3
Normalized emittance (cm·mrad)	<π	<0.6π(at 120 mA, 90 %)	0.3π
Repetition rate (pps)	20	20	
RF power			
Tank excitation (MW)	1	1	
Beam loading (MW)	20 × I(A)		
Frequency (MHz)	201.250	201.078	
RF pluse length (μs)	250		

Operational Performance of the Linac

At the first evacuation of the tank, it took about 6 hours to pump to the pressure of 1×10^{-6} torr. However, after that the pump down time was reduced to less than 4 hours even after exposure to the atmospheric pressure, and any trouble has not been experienced with regard to the vacuum system of the tank.

The electroplated surfaces of the tank and drift-tubes have shown the great advantage to the high power rf excitation. At the first rf feeding, the multipactering levels were instantly broken through and the acceleration power level was attained within an hour. After several sparkings were observed during the first an hour, rf excitation of the tank has been quite stable. It seems due to the smoothness and cleanness of the surfaces. (Fig.1.)

Nevertheless, the sparking patterns similar to the other linacs were found on the surfaces of the first several drift tubes after two years operation.

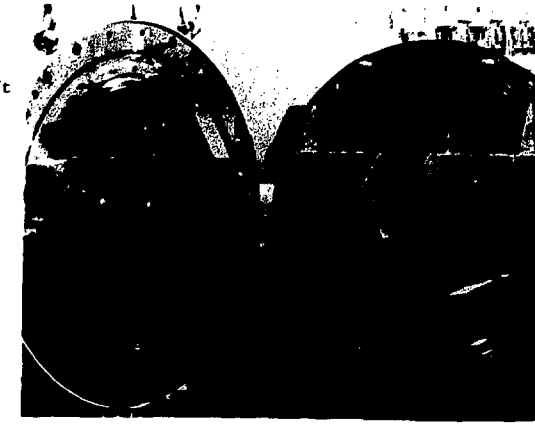

Fig.1 Copper plated tank and drift tubes.

Fig.2 Sparking pattern of the first drift tube.

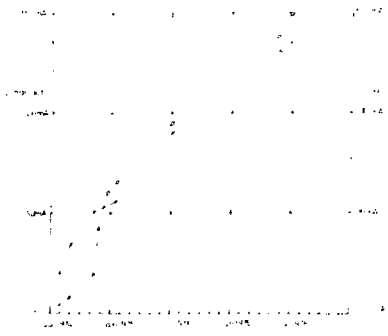

Fig.3 Beam current growth over 2 years.
• input current, ◦ output current

Fig.4 Output beam without compensation
25 mA/div. 5 μs/div.

Fig.5 Output beam with compensation
25 mA/div. 5 μs/div.

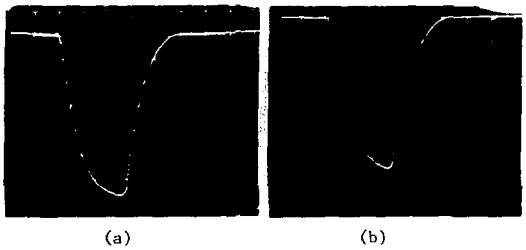

(a) (b)

Fig.6(a),(b) rf power level in tank (50 mA)
(a) without compensation
(b) with compensation

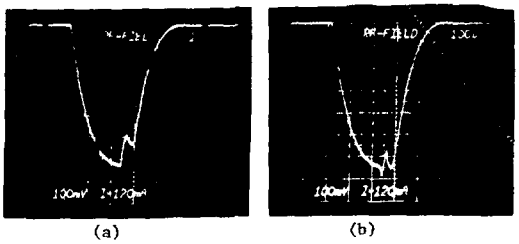

(a) (b)

Fig.7(a),(b) rf power level in tank (120 mA)
(a) without compensation
(b) with compensation

The number of the sparking craters rapidly decreases with gap number and dark colored contaminations inside the bore tubes were found only on the first two drift tubes. It appears that the sparkings are originated from the preinjector.

Since the first acceleration, the beam current level has increased as shown in Fig.3. According to the increase of current, field level decreases because of the beam loading. Consequently, the beam pulse shape droops at the top of the pulse unless the beam loading is compensated. (Fig.4.) However, the droop is remedied by the rf compensation of the beam loading (Fig.5).

For the current level of less than 50 mA, the compensation is completely sufficient by only amplitude modulation. (Fig.6,a,b.)

For heavy loading the compensation becomes insufficient and detuning of tank frequency is needed. (Fig.7a,b). The detuning frequency shifts required for various current levels are shown in Fig.8.

In order to compensate such a heavy loading completely, the phase compensation is necessary in addition to the amplitude compensation. The phase compensation system is now being prepared.

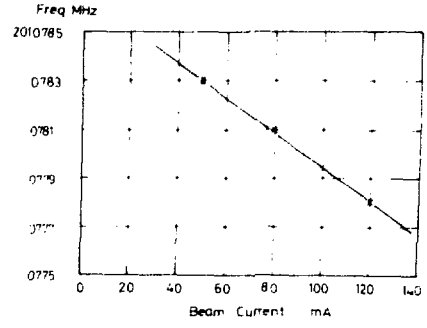

Fig.8 Detuning of tank.

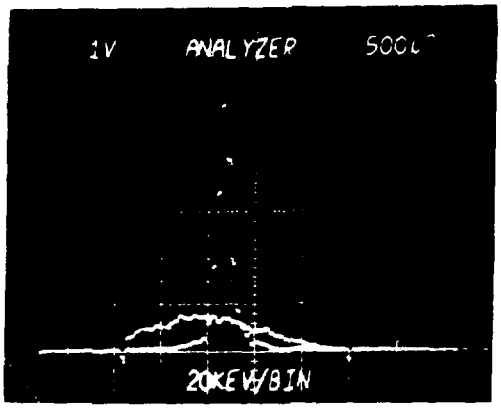

Fig.9 Energy spectra at 120 mA, with and without debuncher. 0.1 %/bin

The debuncher has been operated since Nov.1974. Output beam of the linac has energy spread of ±1.2 percent at the current of 120 mA. The energy spread is reduced to ±0.3 percent by the debuncher. The debuncher is not only efficient for reducing energy spread but for stabilizing of the mean beam energy. By the debuncher, the mean energy stabilized to less than 0.15 percent. Fig.9 shows the typical energy distribution of the beam at the current level of 120 mA.

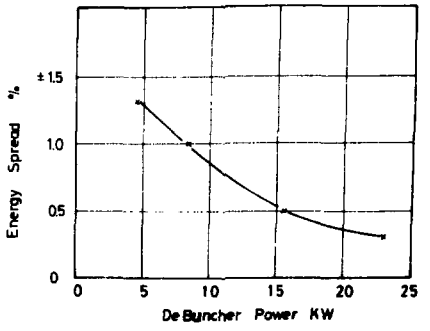

Fig.10 Energy spread versus debuncher rf power.

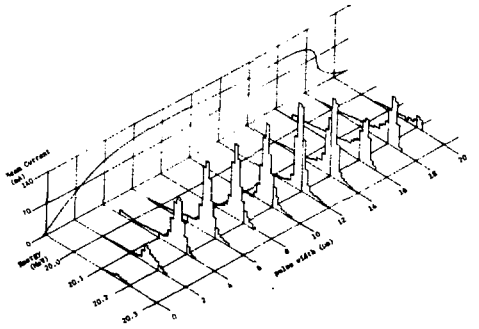

Fig.11 Energy spectra during beam pulse width.

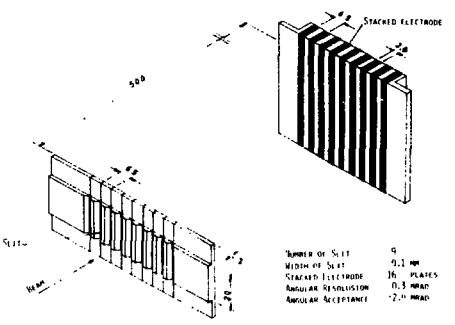

Fig.12 Multi-slit emittance monitor.

The energy spread is variable by adjusting the rf power level of debuncher as shown in Fig.10 and it is possible to reduce the spread up to ±0.2 percent at the current level of less than 100 mA.

Fig.11 shows a variation of the energy spectrum during pulse length of 17 μs. The mean energy is variable within a range of ±0.5 percent by phasing input rf power of the debuncher, keeping the energy distribution unchanged.

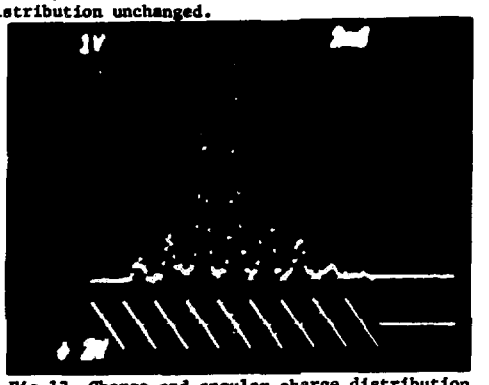

Fig.13 Charge and angular charge distribution measured by multi-slit emittance monitor.

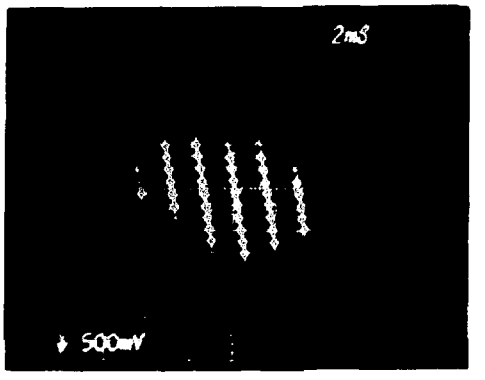

Fig.14 90 % emittance pattern (120 mA)

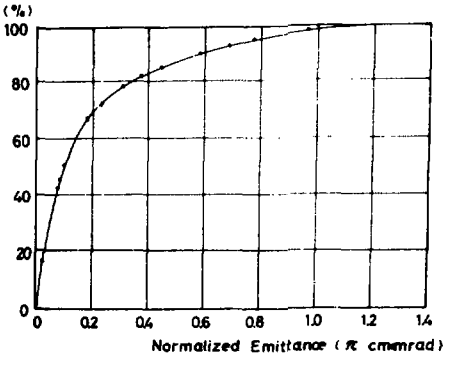

Fig.15 Percentages of beam versus emittance

Emittance of the beam is measured by the multi-slit emittance monitor which consists of 9 slits and the corresponding 9 stacked multi-channel pick-up units as shown in Fig.12. Each unit consists of 16 insulated electrodes.

By the monitor, horizontal distribution and horizontal angular distribution of the beam are measured at the same time. The distribution and the emittance space area are displayed on scopes and the area is variable according to percentage of the incident current. (Fig.13, 14)

Aspect of the normalized emittance for the various percentages of the beam is shown in Fig.15. However, the emittance of the linac is strongly depend on the emittance of the preinjector.

Tilting of the Field Distribution[1]

The designed average field distribution of the KEK linac is given by

$$E_{Z0} = 1.5 + 0.04\ Z(MV/m)$$

where Z is the distance along the axis.

The field distribution was adjusted by 14 tuners so as to fit the designed value as possible.[2]

These tuners are also available to tilt the field distribution. The field distribution is tilted linearly along the tank axis by inserting the first two or the last two tuners.

Inserting the first two tuners into the tank, the field raises linearly along the axis and by last two tuners the field falls linearly. The slope is linear with the insertion of the tuners.

At a specified slope the beam was accelerated and the energy, energy spread and the tramsmitted current were measured for the various rf power levels.

The tank field distributions of respective slopes were measured for the respective optimum spread.(Fig.16)

According to the experiment, the field distributions for the optimum energy spread were expressed by

$$E_Z = E_{Z0} \cdot f(z)$$

$$f(Z) = 1 + \alpha\left(\frac{2Z}{L} - 1\right)$$

where L is the length of the tank and α is the slope of field distribution.

This shows that the field at the output end is increased by α and decreased by α at the input end with respect to the original distribution E_{Z0}.

The results of the experiment are concluded as follows:

1. The effects on the energy spread were not remarkable.

2. A maximum of the mean energy appeared as changing the field level for the respective slopes.

The calculation shows similar results to the experiment. (Fig.18, 19)

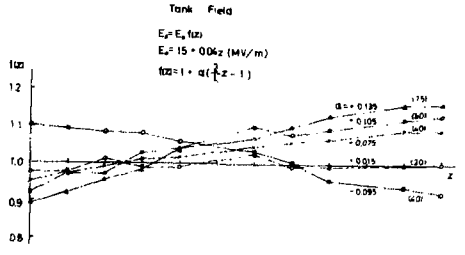

Fig.16 Measured field ditributions at optimum energy spread for various slopes.

References

(1) K. Batchelor et al., Proc. of the 1972 Proton Linear Accelerator Conference p.41.

G.W. Wheeler, Proc. of the U.S.-Japan Seminar on High Energy Acc. Science, Nov.1973, p.269.

(2) S.Okumura and D. Swenson, KEK-74-15, Mar. 1975

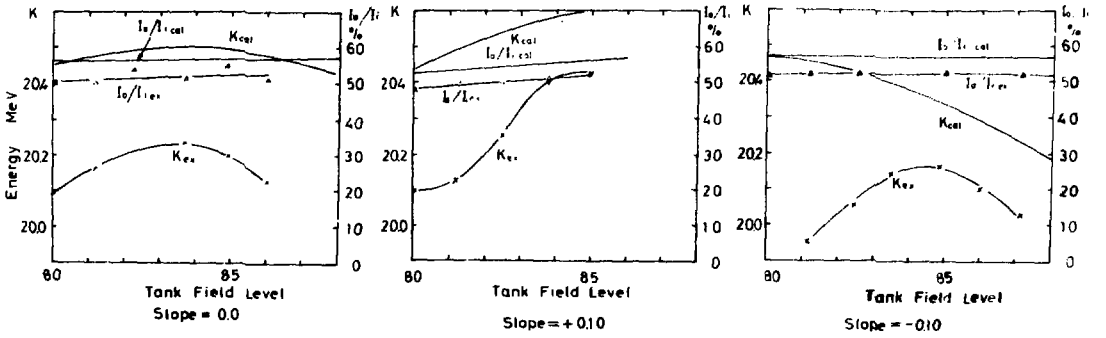

Fig.17 Variations of mean energy and transmitted currents versus tank field level at various field slopes.

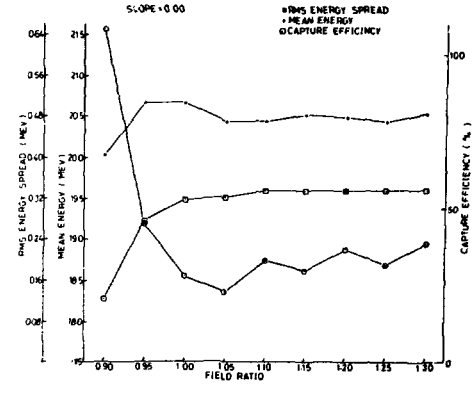

(a)

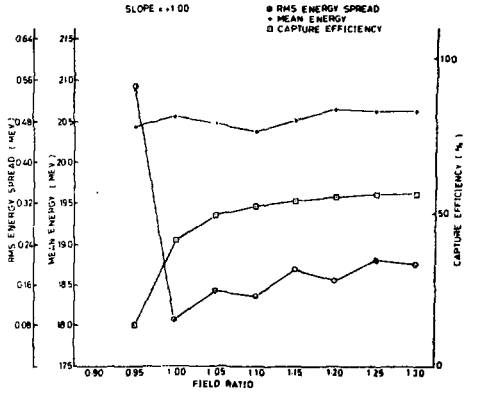

(b)

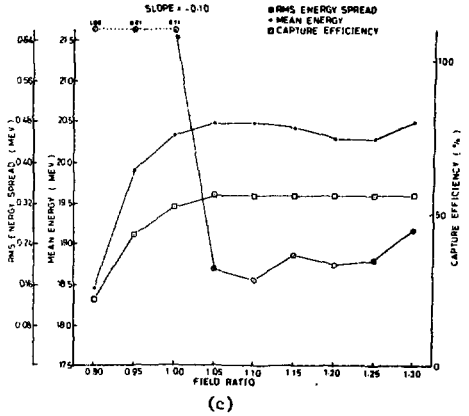

(c)

Fig.18 (a) (b) (c)
Calculated mean energy, rms energy spread and capture efficiency versus tank field level at various slopes.

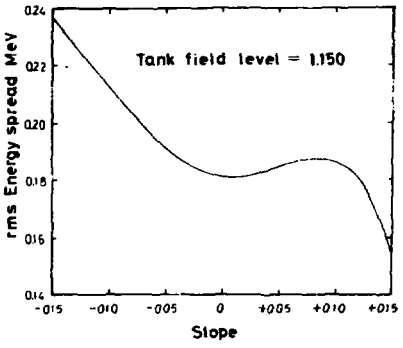

Fig.19 Energy spread versus slope of field (calculated).